

The impact of pulse duration on composite WATERGATE pulse

Jingjing Wang^{a,b}, Xu Zhang^{a,*}, Peng Sun^{a,b}, Xianwang Jiang^{a,b}, Bin Jiang^a, Chunyang Cao^c, Maili Liu^{a,**}

^aState Key Laboratory of Magnetic Resonance and Atomic and Molecular Physics, Wuhan Institute of Physics and Mathematics, Chinese Academy of Sciences, Wuhan 430071, China

^bGraduate School of Chinese Academy of Sciences, Beijing 100049, China

^cShanghai Institute of Organic Chemistry, Chinese Academy of Sciences, Shanghai 200032, China

ARTICLE INFO

Article history:

Received 5 April 2010

Revised 8 July 2010

Available online 16 July 2010

Keywords:

Solvent suppression

WATERGATE

RF pulse

Chemical shift evolution

ABSTRACT

As an effective method for solvent suppression, WATERGATE is widely used in high resolution NMR spectroscopy. It is usually composed of a number of pulses separated by constant intervals. However, theoretical and experimental analyses indicate that narrower bandwidth and lower intensities around the secondary suppression points occur in the excitation profile of the composite WATERGATE. The excitation profile distortion is caused by the chemical shift evolution during the RF pulses. The higher the ratio of pulse duration to the inter-pulse delay is, the severer the profile distorts. Therefore, in high magnetic fields, the effect will be serious when WATERGATE is applied to some biological samples whose resonances distribute over a wide range. As can be seen obviously by applying WATERGATE to detect a RNA–protein mixture sample in an 800 MHz spectrometer, the resonances of the imino protons were partially suppressed by showing decreased intensities, though the intended secondary suppression points were set far away from them. In this article, we proposed an optimized WATERGATE that could effectively compensate the chemical shift evolution during the RF pulses, and relieve the excitation profile distortion. The optimized experiment will be a good way to retain the imino signal intensities when WATERGATE is applied to detect the RNA samples in high magnetic field.

© 2010 Elsevier Inc. All rights reserved.

1. Introduction

NMR spectroscopy is a powerful tool in biology, and has been widely used in studies of biomolecular structure and dynamics. In biological NMR, the suppression of water is essential, because the signal intensity of H₂O is much higher than that of solute. A lot of techniques have been proposed for solvent suppression [1–33]. Among these methods, WATERGATE [17–19] is one of the most prevailing methods, which assembles spin-echo pulse sequence with selective pulses or pulse train flanked by two symmetrical gradient pulses. The pulse sequence can be a non-selective π pulse sandwiched by two selective $\pi/2$ pulses [17], or a selective composite pulse train, such as W3 [18] and W5 [19]. The usual form of the composite pulse is $\alpha_1(x) - \tau - \alpha_2(x) - \tau \dots - \alpha_n(x) - \tau - \alpha_n(-x) \dots - \tau - \alpha_2(-x) - \tau - \alpha_1(-x)$ [18,19]. Where, α_n are RF pulses with variable duration; x , and $-x$ are the phases of the corresponding pulses; τ is a short inter-pulse delay used to control the null-excitation points or suppression points. In composite pulse WATERGATE, the intended null-excitation points are $1/\tau$ (Hz) apart from each other. However, we noticed there was excitation profile distortion in the experiments of W3 and W5. The distortion was caused by the chemical shift evolution during the RF pulses, which was unfor-

tunately not taken into consideration in the conventional experiment setup.

Taking the pulse train of W3 and W5 as examples, we analyzed the effect of the chemical shift evolution during the RF pulses on the excitation profile. Both simulations and experiments indicated that the excitation profile distortion could be compensated by modifying the inter-pulse delays accordingly.

2. Theory

All the simulations were carried out without considering the effects of J coupling and relaxation. In conventional WATERGATE experiment, when chemical shift evolution during the RF pulse is not considered, the product operator evolutions during each inter-pulse delay τ and pulse α_n are $\exp(i\Omega_z\tau)$ and $\exp(i\theta_n I_x)$, respectively. The elements in these two terms can be written as:

$$\exp(i\Omega_z\tau) = \begin{bmatrix} \cos(\omega\tau) & \sin(\omega\tau) & 0 \\ -\sin(\omega\tau) & \cos(\omega\tau) & 0 \\ 0 & 0 & 1 \end{bmatrix} \quad (1)$$

$$\exp(i\theta_n I_x) = \begin{bmatrix} 1 & 0 & 0 \\ 0 & \cos(m_n\alpha) & \sin(m_n\alpha) \\ 0 & -\sin(m_n\alpha) & \cos(m_n\alpha) \end{bmatrix} \quad (2)$$

* Corresponding author. Fax: +86 27 87199291.

** Corresponding author. Fax: +86 27 87199291.

E-mail addresses: zhangxu@wipm.ac.cn (X. Zhang), ml.liu@wipm.ac.cn (M. Liu).

where $\omega/2\pi$ is frequency offset with respect to center suppression point where the RF pulse carrier frequency is located. τ is the inter-pulse delay, and α is equal to $\pi/26$. For W3 experiment, $n = 1-6$, and $m_n = 3, 9, 19, -19, -9$, and -3 , respectively. For W5 experiment, $n = 1-10$, $m_n = 1.12, 2.67, 5.37, 10.11, 19.38, -19.38, -10.11, -5.37, -2.67$, and -1.12 , respectively. The final signal I_ρ of WATERGATE is:

$$I_\rho = I_{\rho_0} \prod_{n=1}^{N-1} [\exp(i\theta_n I_x) \exp(i\Omega_z \tau)] \exp(i\theta_N I_x) \quad (3)$$

where $I_{\rho_0} = \begin{bmatrix} 0 \\ I_y \\ 0 \end{bmatrix}$, $N = 6$, and 10 for W3 and W5, respectively. Since

W5 is a double spin-echo procedure, those operations should be applied twice.

Fig. 1a shows the simulated excitation profile of W3 without considering the chemical shift evolution during the RF pulses. In such case, the excitation profile is the intended result of WATERGATE, which is widely accepted and always remains the same no matter how much the pulse duration is. The distance (d) between two adjacent suppression points is defined by the inter-pulse delay as $d = 1/\tau$. When the inter-pulse delay is 200 μs , the distance d is 5000 Hz, and is not affected by the change of the pulse duration.

When considering the chemical shift evolution during those pulses, an extra operator $\exp(i\Omega_z T_n)$ has to be introduced into the simulation.

$$\exp(i\Omega_z T_n) = \begin{bmatrix} \cos(\omega m_n p_x) & \sin(\omega m_n p_x) & 0 \\ -\sin(\omega m_n p_x) & \cos(\omega m_n p_x) & 0 \\ 0 & 0 & 1 \end{bmatrix} \quad (4)$$

where p_x is the pulse duration of α . In the simulation, each pulse α_n is divided into 100 small pulses with equal duration. Accordingly, the product operators $\exp(i\theta_n I_x/100)$ and $\exp(i\Omega_z T_n/100)$ for those small pulses can be considered as commuting operators. Therefore, evolution during each pulse in WATERGATE should be $\prod_{i=1}^{100} (\exp(i\theta_n I_x/100) \exp(i\Omega_z T_n/100))$. With this extra chemical shift evolution, the resulted signal I_ρ becomes:

$$I_\rho = I_{\rho_0} \prod_{n=1}^{N-1} \left[\left(\prod_{i=1}^{100} (\exp(i\theta_n I_x/100) \exp(i\Omega_z T_n/100)) \right) \exp(i\Omega_z \tau) \right] \times \prod_{i=1}^{100} \exp(i\theta_N I_x/100) \quad (5)$$

The corresponding simulated excitation profiles of W3 with different pulse durations are shown in Fig. 1b. Although the excitation profiles around the center suppression point are similar to the intended results shown in Fig. 1a, the profiles around the secondary suppression points show clear RF pulse duration dependent after considering the chemical shift evolution. The secondary suppression points move towards the center point gradually with the increase of pulse duration. For $\pi/2$ pulse of 10 μs and 30 μs , their distances decrease 250 Hz and 750 Hz, respectively. In addition, the signal intensities at the secondary suppression regions are reduced, especially when the pulse duration is longer. This is reasonable, because the pulse duration provides an extra time for chemical shift evolution. Therefore, the higher the ratio of pulse duration to the inter-pulse delay is, the more serious the excitation profile distortion becomes.

In order to relieve the excitation profile distortion in WATERGATE mentioned above, the chemical shift evolution during the RF pulses has to be considered. It was reported that a pulse in duration of pw could be approximately treated as an ideal pulse preceded and followed by an evolution period $2pw/\pi$ [34]. Therefore, the i th inter-pulse delay in WATERGATE should be set to $\tau'_i = \tau - 2(pw_i + pw_{i+1})/\pi$, where, pw_i and pw_{i+1} are the pulse durations before and after the delay τ'_i , respectively. Obviously, the inter-pulse delays are variant and pulse dependent.

For comparison, Fig. 1c shows the simulated excitation profiles of W3 with optimized inter-pulse delays. Three excitation profiles with different pulse durations were simulated. The excitation profiles with optimized parameters are much closer to the intended ones in Fig. 1a. The drift of the secondary suppression point is reduced to 30 Hz for $\pi/2$ pulse of 30 μs , and the signal intensity distortion is significantly relieved as well.

Double WATERGATE utilizes excitation sculpting feature and provides higher suppression efficiency, better baseline and line shape [7,19]. Accordingly, we simulated the excitation profiles of double W5 with and without the compensation of the chemical shift evolution during the RF pulses, and showed the results in Fig. 2. Compare with the intended excitation profile (Fig. 2a), the signal intensities around the secondary suppression points of conventional W5 are significantly dependent on the pulse duration (Fig. 2b). Unlike single W3 (Fig. 1b), the drift of the secondary suppression points is much small for double W5, because it takes the advantage of double spin-echo or excitation sculpting [7,19]. When the chemical shift evolution during the RF pulses is compensated (Fig. 2c), the excitation profile of double W5 is dramatically improved.

3. Results and discussion

To confirm the simulation, excitation profiles of the conventional and optimized WATERGATE were measured using the residual signal of HOD (in D_2O). The experimental excitation profiles of W3 and double W5 are shown in Figs. 3 and 4, respectively. The $\pi/2$ pulse durations are labeled in the figure. Obviously, the experimental profiles are in good agreement with the simulated ones. As expected, the main suppression regions settle in the center, and do not change distinctly, no matter which pulse train is used, or how much the pulse duration is. However, as the pulse duration increases, the secondary suppression regions of the conventional experiments (Figs. 3a and 4a) move towards the main suppression point, resulting in narrower excitation bandwidth and distorted

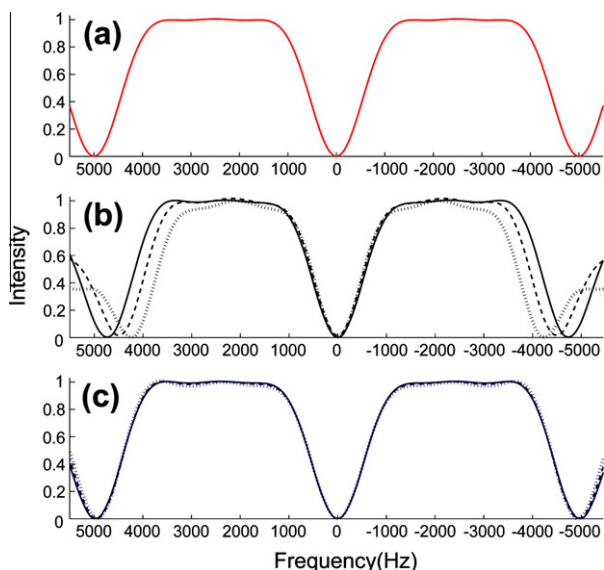


Fig. 1. Simulated excitation profiles of WATERGATE W3 without (a) and with (b) considering the chemical shift evolution during the RF pulses, and the one with optimized inter-pulse delays (c). In all simulations, the original inter-pulse delay (τ) was 200 μs corresponding to inter-suppression points of 5000 Hz. In the optimized experiments, the actual inter-pulse delays were τ'_i , which were defined as $\tau - 2(pw_i + pw_{i+1})/\pi$. The $\pi/2$ pulse duration of 10.0 μs , 20.0 μs and 30.0 μs were simulated, and represented by solid line, dashed line, and dotted line, respectively.

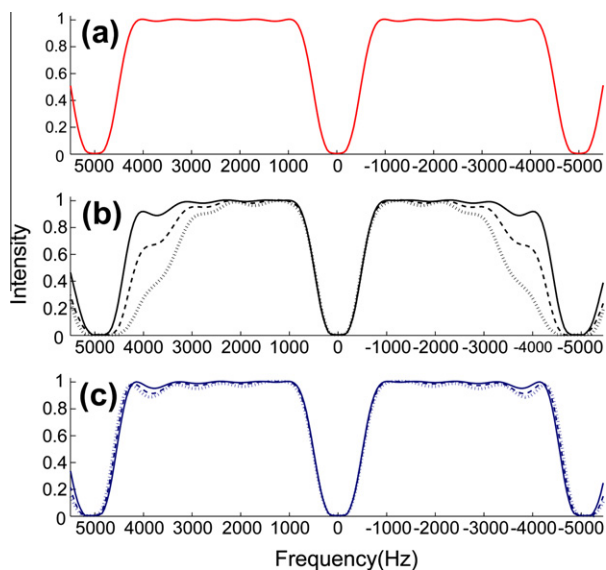


Fig. 2. Simulated excitation profiles of WATERGATE W5 without (a) and with (b) consideration of chemical shift evolution during the RF pulses, and the one with optimized inter-pulse delays (c). In all simulations, the original inter-pulse delay (τ) was 200 μ s corresponding to inter-suppression points of 5000 Hz. In the optimized experiments, the actual inter-pulse delays were τ'_i , which were defined as $\tau - 2(pw_i + pw_{i+1})/\pi$. The $\pi/2$ pulse duration of 10.0 μ s, 20.0 μ s and 30.0 μ s were simulated, and represented by solid line, dashed line, and dotted line, respectively.

signal intensities. In the optimized experiments (Figs. 3b and 4b), the excitation profiles are nearly independent of the pulse width. The results demonstrate that the chemical shift evolution during the RF pulses can be effectively compensated by inter-pulse delay optimization.

The theoretical simulations and experiments indicate that the chemical shift evolution during the RF pulses causes excitation

profile distortion in WATERGATE, especially at the secondary suppression regions. The distortion is pulse duration or ratio of pulse duration to inter-pulse delay dependent. When the pulse duration is short enough, the distortion may be ignored. However, the distortion may become serious if the inter-pulse delay τ is short or the RF pulse duration is long, which can be a frequently encountered problem when WATERGATE is applied in high magnetic field spectrometer. This distortion or problem can be relieved simply by taking the effective evolution time during the RF pulse into account, and adjusting the inter-pulse delay accordingly.

In order to evaluate the optimization, WATERGATE was applied to a RNA–protein mixture sample, and two sets of 800 MHz ^1H NMR spectra (W3 and double W5) were recorded with and without inter-pulse delay optimization, respectively. The $\pi/2$ pulse of 10 μ s and inter-pulse delay of 130 μ s were used in the experiments. This gave rise to the secondary suppression points to be 7692 Hz or 9.61 ppm away from the center one at 4.70 ppm. The results are shown in Fig. 5, where spectral regions from 12.20 ppm to 13.40 ppm are plotted as inserts after vertical scale enlargement. As expected, most of the resonances are the same in each set of WATERGATE experiments, such as the signals between 0.00–4.00 ppm, and 5.70–10.00 ppm, since they are located in center part of the excitation profile at either side of the main suppression point. However, compare with the optimized experiments, the signal intensities of the imino protons between 12.20 ppm and 13.20 ppm are attenuated in the conventional WATERGATE. Since these peaks are close to the intended secondary suppression point at 14.31 ppm, the signal attenuation indicates that those signals are partially suppressed because of the excitation profile distortion in the conventional WATERGATE experiment. Whereas, the high signal intensities of the imino protons in the optimized experiment suggest that the optimization is a good way to retain the signals intensities. Although double W5 provides narrow solvent suppression region, it causes attenuation for broad peaks. This is reasonable because it uses twice the spin-echo time and an extra pair of gradients, which give rise to spin–spin relaxation and self-diffusion.

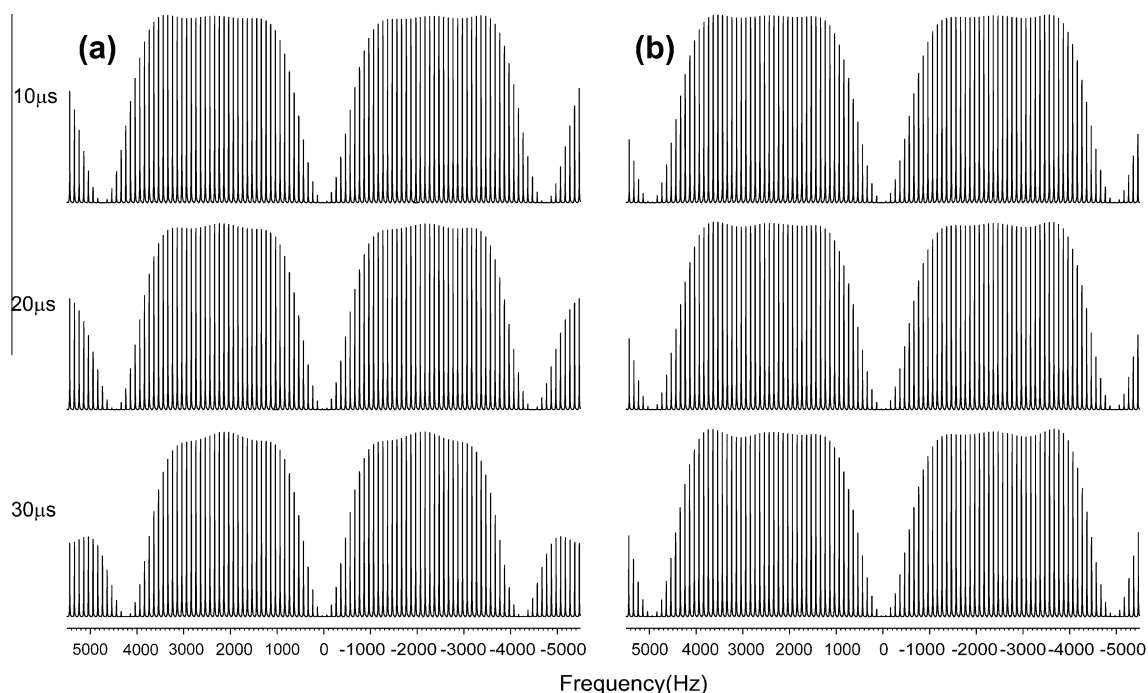


Fig. 3. Experimental excitation profiles of W3 without (a) and with (b) inter-pulse delay optimization. The corresponding $\pi/2$ pulse duration was labeled at the left side of the corresponding excitation profile. The other experiment parameters were the same as those used in Figs. 1 and 2.

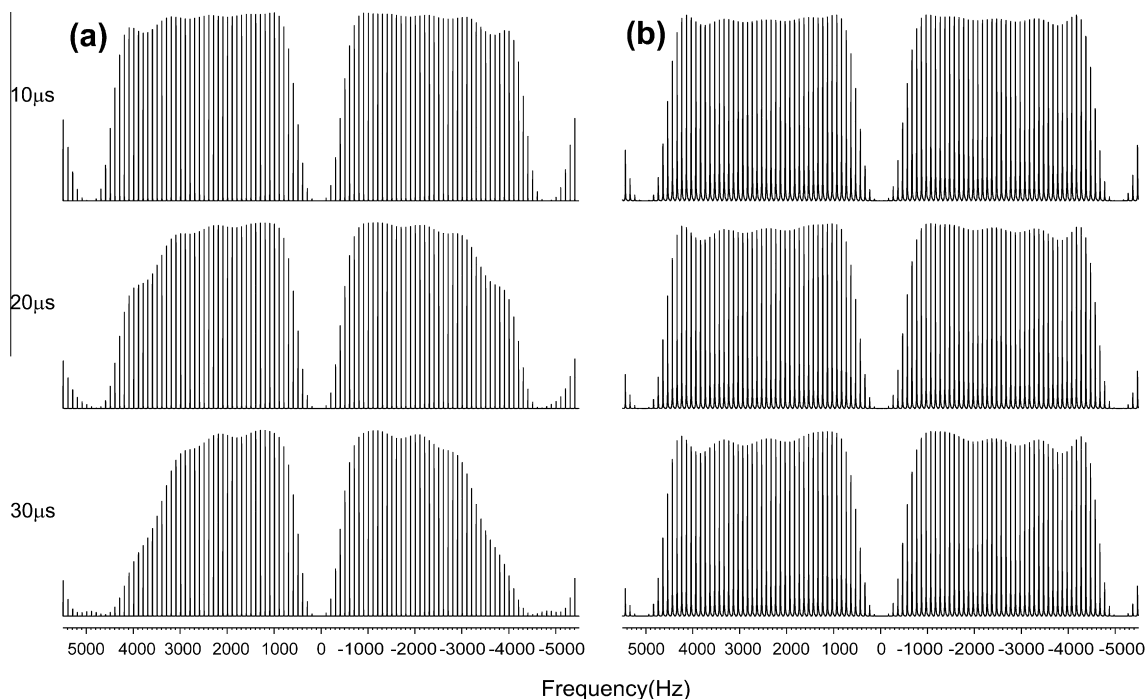


Fig. 4. Experimental excitation profiles of W5 without (a) and with (b) inter-pulse delay optimization. The corresponding $\pi/2$ pulse duration was labeled at the left side of the corresponding excitation profile. The other experiment parameters were the same as those used in Figs. 1 and 2.

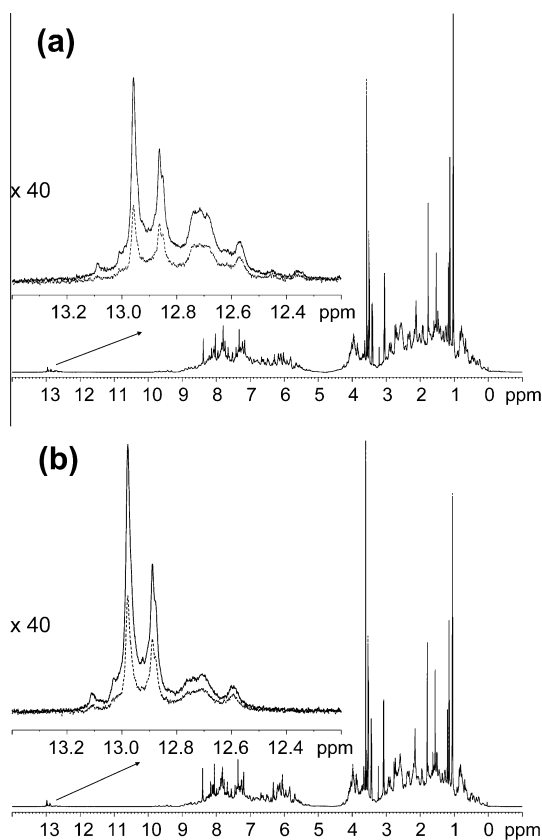


Fig. 5. 800 MHz ^1H NMR spectra of a RNA-protein mixture in water (1.0 mM Bk12, 1.0 mM EF57, 90% H_2O + 10% D_2O) obtained using W3 (a) and double W5 (b). The dashed and solid lines are spectra recorded using the conventional and optimized pulse sequence, respectively. The $\pi/2$ pulse was 10.0 μs , the original inter-pulse delay (τ) was 130 μs . In the optimized experiments, the actual inter-pulse delays were τ'_i , which were defined as $\tau - 2(pw_i + pw_{i+1})/\pi$.

4. Conclusion

In summarization, the theoretical simulation and experimental results indicate that the conventional WATERGATE with composite pulse suffers signal distortion at the secondary suppression regions. The distortion is caused by the chemical shift evolution during the RF pulse, and can be relieved by optimizing the inter-pulse delays accordingly. This is especially important when the experiment is applied to biological samples in high magnetic fields, such as RNA solutions.

5. Materials and experiments

The WATERGATE spectra of HOD in D_2O were all obtained at 298 K on a Bruker AVANCE 500 spectrometer, the corresponding ^1H frequency was 500.13 MHz.

In WATERGATE experiments, the gradients used were 1 ms sine-shaped gradients, each followed by a 200 μs delay for gradient recovery. All the other experiment parameters were kept the same as those used in simulation: the original inter-pulse delay (τ) was 200 μs corresponding to d of 5000 Hz, the $\pi/2$ pulse durations were 10 μs , 20 μs and 30 μs , respectively. In the optimized experiment, the actual inter-pulse delays were τ'_i , which were defined as $\tau - 2(pw_i + pw_{i+1})/\pi$. The experimental excitation profiles were measured in the one-dimensional mode by shifting the carrier frequency in a step of 100 Hz for each scan.

To test the optimized WATERGATE W3 and W5, a RNA-protein mixture sample was prepared in water (1.0 mM Bk12, 1.0 mM EF57, 90% H_2O + 10% D_2O), non-optimized and optimized W3 and double W5 spectra were recorded on a Bruker AVANCE III 800 spectrometer with $\pi/2$ pulse of 10 μs . The original inter-pulse delay τ of 130 μs was used corresponding to d of 7692 Hz. The carrier frequency was set at 4.70 ppm, which is on-resonance of water signal. In the optimized experiment, the actual inter-pulse delays were τ'_i , which were defined as $\tau - 2(pw_i + pw_{i+1})/\pi$. The strengths

of the gradient pulses were 10 G/cm for W3, and 17 G/cm and 11 G/cm for double W5, respectively.

Acknowledgments

The authors thank Dr. Daiwen Yang and the anonymous reviewers for their constructive suggestion. This research is supported by grants from National Natural Science Foundation of China (Nos. 20875098, 20635040, 20921004), National Major Basic Research Program of China (No. 2009CB918603), and the Ministry of Science and Technology of China (2009IM030700).

References

- [1] M. Guéron, P. Plateau, M. Decorps, Solvent signal suppression in NMR, *Prog. Nucl. Magn. Reson. Spectrosc.* 23 (1991) 135–209.
- [2] W.S. Price, Water signal suppression in NMR spectroscopy, in: G.A. Webb (Ed.), *Annual Reports on NMR Spectroscopy*, vol. 38, London, 1999, pp. 289–354.
- [3] G. Zheng, W.S. Price, Solvent signal suppression in NMR, *Prog. Nucl. Magn. Reson. Spectrosc.* 56 (2010) 267–288.
- [4] M. Guéron, P. Plateau, A. Kettani, M. Decorps, Improvements in solvent-signal suppression, *J. Magn. Reson.* 96 (1992) 541–550.
- [5] A.S. Altieri, R.A. Byrd, Randomization approach to water suppression in multidimensional NMR using pulsed-field gradients, *J. Magn. Reson. B* 107 (1995) 260–266.
- [6] J. Brondeau, P. Mutzenhardt, J.M. Tyburn, D. Canet, Improved water elimination in NOESY experiments by radiofrequency field gradients, *J. Magn. Reson. B* 109 (1995) 310–313.
- [7] T.L. Hwang, A.J. Shaka, Water suppression that works. Excitation sculpting using arbitrary wave-forms and pulsed-field gradients, *J. Magn. Reson. A* 112 (1995) 275–279.
- [8] R.J. Ogg, P.B. Kingsley, J.S. Taylor, WET, a T_1 - and B_1 -insensitive water-suppression method for in vivo localized ^1H NMR spectroscopy, *J. Magn. Reson. B* 104 (1994) 1–10.
- [9] S.H. Smallcombe, S.L. Patt, P.A. Keifer, WET solvent suppression and its applications to LC NMR and high-resolution NMR spectroscopy, *J. Magn. Reson. A* 117 (1995) 295–303.
- [10] H. Mo, D. Raftery, Improved residual water suppression: WET180, *J. Biomol. NMR* 41 (2008) 105–111.
- [11] S. Zhang, X. Yang, D.G. Gorenstein, Enhanced suppression of residual water in a “270” WET sequence, *J. Magn. Reson.* 143 (2000) 382–386.
- [12] I.M. Brereton, G.J. Galloway, J. Field, M.F. Marshman, D.M. Doddrell, Gradient-induced water-suppression techniques for high-resolution NMR-spectroscopy, *J. Magn. Reson.* 81 (1989) 411–417.
- [13] G.M. Clore, B.J. Kimber, A.M. Gronenborn, The 1–1 hard pulse – a simple and effective method of water resonance suppression in FT ^1H -NMR, *J. Magn. Reson.* 54 (1983) 170–173.
- [14] S.C. Sahu, A. Majumdar, Pulsed-field gradient-based water suppression techniques in homonuclear NMR spectroscopy, *Curr. Sci.* 74 (1998) 451–456.
- [15] A.D. Gossert, C. Henry, M.J.J. Blommers, W. Jahnke, C. Fernández, Time efficient detection of protein-ligand interactions with the polarization optimized PO-WaterLOGSY NMR experiment, *J. Biomol. NMR* 43 (2009) 211–217.
- [16] M.M. Hoffmann, H.S. Sobstyl, S.J. Seedhouse, T_1 relaxation measurement with solvent suppression, *Magn. Reson. Chem.* 46 (2008) 660–666.
- [17] M. Piotto, V. Saudek, V. Sklenar, Gradient-tailored excitation for single-quantum NMR-spectroscopy of aqueous-solutions, *J. Biomol. NMR* 2 (1992) 661–665.
- [18] V. Sklenar, M. Piotto, R. Leppik, V. Saudek, Gradient-tailored water suppression for ^1H - ^{15}N HSQC experiments optimized to retain full sensitivity, *J. Magn. Reson. A* 102 (1993) 241–245.
- [19] M. Liu, X.A. Mao, C. Ye, H. Huang, J.K. Nicholson, J.C. Lindon, Improved WATERGATE pulse sequences for solvent suppression in NMR spectroscopy, *J. Magn. Reson.* 132 (1998) 125–129.
- [20] P.C.M. van Zijl, C.T.W. Moonen, Complete water suppression for solutions of large molecules based on diffusional differences between solute and solvent (DRYCLEAN), *J. Magn. Reson.* 87 (1990) 18–25.
- [21] C.T.W. Moonen, P.C.M. van Zijl, Highly effective water suppression for in vivo proton NMR-spectroscopy (Drysteam), *J. Magn. Reson.* 88 (1990) 28–41.
- [22] S. Grzesiek, A. Bax, The importance of not saturating H_2O in protein NMR. Application to sensitivity enhancement and NOE measurements, *J. Am. Chem. Soc.* 115 (1993) 12593–12594.
- [23] D.L. Mattiello, W.S. Warren, L. Mueller, B.T. Farmer II, Minimizing the water resonance in biological NMR: characterization and suppression of intermolecular dipolar interactions by multiple-axis gradients, *J. Am. Chem. Soc.* 118 (1996) 3253–3261.
- [24] W.S. Price, Y. Arata, The manipulation of water relaxation and water suppression in biological systems using the Water-PRESS pulse sequence, *J. Magn. Reson. B* 112 (1996) 190–192.
- [25] W.S. Price, K. Hayamizu, Y. Arata, Optimization of the Water-PRESS pulse sequence and its integration into pulse sequences for studying biological macromolecules, *J. Magn. Reson.* 126 (1997) 256–265.
- [26] W.S. Price, F. Elwinger, C. Vigouroux, P. Stilbs, PGSE-WATERGATE, a new tool for NMR diffusion-based studies of ligand-macromolecule binding, *Magn. Reson. Chem.* 40 (2002) 391–395.
- [27] G. Zheng, T. Stait-Gardner, P.G. Anil Kumar, A.M. Torres, W.S. Price, PGSTE-WATERGATE: an STE-based PGSE NMR sequence with excellent solvent suppression, *J. Magn. Reson.* 191 (2008) 159–163.
- [28] W.S. Price, M. Walchli, NMR diffusion measurements of strong signals: the PGSE-Q-switch experiment, *Magn. Reson. Chem.* 40 (2002) S128–S132.
- [29] K.I. Momot, P.W. Kuchel, Convection-compensating PGSE experiment incorporating excitation-sculpting water suppression (CONVEX), *J. Magn. Reson.* 169 (2004) 92–101.
- [30] A.J. Simpson, S.A. Brown, Purge NMR: effective and easy solvent suppression, *J. Magn. Reson.* 175 (2005) 340–346.
- [31] G. Zheng, A.M. Torres, W.S. Price, Solvent suppression using phase-modulated binomial-like sequences and applications to diffusion measurements, *J. Magn. Reson.* 194 (2008) 108–114.
- [32] B.D. Nguyen, X. Meng, K.J. Donovan, A.J. Shaka, SOGGY: solvent-optimized double gradient spectroscopy for water suppression. A comparison with some existing techniques, *J. Magn. Reson.* 184 (2007) 263–274.
- [33] G. Zheng, W.S. Price, Simultaneous convection compensation and solvent suppression in biomolecular NMR diffusion experiments, *J. Biomol. NMR* 45 (2009) 295–299.
- [34] J. Cavanagh, W.J. Fairbrother, A.G. Palmer III, M. Rance, N.J. Skelton, *Protein NMR Spectroscopy: Principles and Practice*, second ed., Elsevier Academic Press, Burlington, MA, 2007.